LOADED CARBON COMPOSITE SCARF JOINTS SUBJECT TO QUASI STEADY LATERAL LOADS

Henry C. H. Li*, Stefanie Feih*, Andrew J. Gunnion, Israel Herszberg** and Murray L. Scott****

***School of Aerospace, Mechanical and Manufacturing Engineering, RMIT University, GPO Box 2476V, Melbourne, VIC 3001, Australia.**

****Cooperative Research Centre for Advanced Composite Structures Limited 506 Lorimer Street, Fishermans Bend, Victoria, 3207, Australia.**

Keywords: *Carbon composite, bonded repair, scarf joint, impact*

Abstract

A study was conducted to assess the strength of carbon epoxy composite panels incorporating a 5° scarf joint under various levels of tensile prestrain, subjected to a quasi-static lateral force. This lateral force was intended to simulate an impact event, where quasi-static loading was applied instead of a dynamic impact load to remove the effect of strain rate on the adhesive properties.

An experimental investigation indicated that the failure load was significantly different for a range of in-plane prestrains between 0 and 4,000 με. This was due to the change in bending stiffness of the structure as a result of the prestrain. Finite element modelling was conducted to validate the experimental results. The experimental results correlated well with the theoretical findings. The implications of this study in relation to the impact behaviour of scarf repairs are also discussed.

1 Introduction

Scarf repairs are commonly used to repair heavily loaded composite aerospace structures. Not only do they provide efficient load transfer and hence high strength recovery, scarf patches also produce minimal surface disturbances which is important for aerodynamic and stealth considerations. Significant cost savings may be realised compared to the alternative of component replacement [1].

Bonded repairs on the external surface of an aircraft are subject to the same impact risks as those of the parent structure. Consequently, an understanding of the impact response and tolerance of such repairs is essential to enable the assessment of their effectiveness and durability.

The impact resistance of polymer laminates has been a topic of intensive investigation for many years. Comprehensive reviews on this subject matter have been produced by Abrate [3] and Reid et al. [4]. Much of the impact studies on composite structures, reported in the literature, have been conducted with the impact taking place on unloaded structures. This however, does not truly represent events likely to be encountered in service, such as runway debris impact and bird strikes. In the limited literature on the impact of prestrained composite structures, it has been reported that catastrophic failure was found to occur in cases when the panels were impacted at levels which when applied to the unloaded panels did not reduce significantly their residual strength [3].

Previous studies conducted by the authors on loaded impact of scarf joints postulated that the behaviour was heavily influenced by the strain rate sensitivity of the adhesive [5,6]. This paper examines the behaviour of similar composite bonded scarf patch systems to a lateral load representative of an impact event.

The lateral loading was applied quasi-statically so that the effect of adhesive strain rate sensitivity could be eliminated, allowing the mechanics of the complex loading configuration to be examined. A 5° scarf joint in a 3.2 mm thick, quasi-isotropic carbon epoxy panel was considered. This is representative of a common flush structural repair. The failure mechanisms of these joints under a range of tensile prestrains (0 - 4,000 με) were determined using finite element (FE) modelling and experimental testing. The findings are discussed in relation to impact loading.

2 The Scarf Joint

A typical scarf joint is shown in Figure 1. The scarf joint is engineered such that it restores the full design ultimate strength of the parent structure [7]. In order to achieve this, a very shallow scarf angle is normally used so that the adhesive shear stress is kept low.

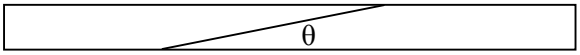

Figure 1: Cross-section of a scarf joint

The allowable scarf angle may be calculated using the following expression [7]:

$$\theta \leq \frac{\tau_{adh}}{\varepsilon_u E} \qquad (1)$$

Where θ is the scarf angle in radians, τ_{adh} is the adhesive shear strength, ε_u and E are the design ultimate strain and modulus of the parent structure. Note that this formulation is based on a 2-D full-width scarf joint where load bypass is not available, and is hence conservative.

Using a high-performance film adhesive with a hot-wet (105°C, 100% relative humidity) strength of 20 MPa, bonded to a carbon/epoxy parent structure with a design ultimate strain of 4,000 με and modulus of 70 GPa, the maximum scarf angle can be calculated to be 4°. However, a larger scarf angle may be used due to load bypass around the repaired region, and particularly if the stringent hot-wet condition is not required. It is desirable to use the largest possible scarf angle in order to minimise the amount of material which needs to be removed from the parent structure.

Based on FE analyses, Soutis and Hu [8] have reported that the angle for the composite scarf repair, which they examined, could be increased from 4° to almost 7° when the effect of bypass was included in the model.

In this study, a 5° scarf angle was used and all mechanical tests were conducted under laboratory controlled room temperature-dry conditions. Furthermore, it considered unlikely that impact of repairs would occur under the hot-wet condition with no structural load bypass available.

3 Experimental Study

3.1 Specimen Design and Manufacture

A quasi-isotropic carbon/epoxy panel was used as the precursor for the manufacture of the scarf joint specimens. The material used was the Cycom T300/970 177°C cure prepreg system with a ply thickness of 0.2 mm. The lay-up sequence was $[45\ 90\ -45\ 0]_{2s}$ which yielded a nominal panel thickness of 3.2 mm. This was considered representative of typical composite aerospace structures.

The dimensions of the test specimens were 50 mm wide by 205 mm long. The scarf joints were machined in a computer numerically controlled mill and bonded using FM73 structural film adhesive with a nominal thickness of 0.38 mm. The total length of the bondline was approximately 37 mm. The adhesive was cured at 120°C for 2 hours under a 1 atmosphere vacuum.

3.2 Testing

A 100 kN MTS hydraulic test machine was used to apply a tensile preload to the test specimens. The preload introduced corresponding prestrains of 0, 1,000, 2,000, 3,000 and 4,000 με. The prestrains were determined from calibration specimens with surface attached extensometers. The specimen gauge length was 140 mm.

A test rig was developed to apply lateral loading at the centre of the scarf joint whilst keeping the in-plane load constant. The lateral

force was introduced using a threaded steel rod and reacted against the ends of the test specimen. Consequently, the tensile test machine used to apply the in-plane loading was undisturbed by the lateral force. A photograph of the test set-up is shown in Figure 2.

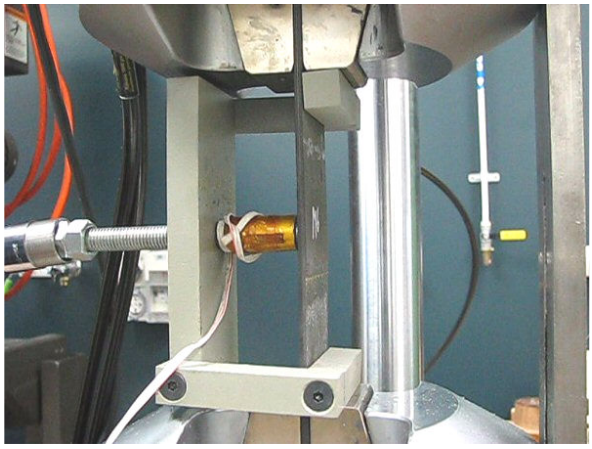

Figure 2: Test set-up

In order to simulate an impact event, a 12 mm diameter steel ball was installed at the top of the loading rod. The ball and the rod were connected via a small length of aluminium tube filled with epoxy adhesive. A strain gauge was attached to the outside wall of the aluminium connecting tube and calibrated against the applied load in a separate test machine. This allowed the measurement of the lateral force. The lateral displacement was measured from the number of revolutions of the loading rod and the thread pitch and calibrated against a dial gauge.

The scarf joint specimens were tested to failure in lateral loading at each in-plane prestrain level. The lateral failure loads and displacements were recorded and the specimen failure mechanisms were examined.

3.3 Test Results

The experimental results are summarised in Table I. It is apparent that the bending stiffness of the specimen increased significantly with increasing prestrain. The lateral failure load was found to be the highest at a tensile prestrain of 2,000 με.

Table I: Experimental results

Tensile Prestrain (με)	Lateral Failure Load (N)	Bending Stiffness (N/mm)
0	1,596	212.2
1,000	4,267	381.6
2,000	4,967	591.9
3,000	4,537	726.5
4,000	3,788	795.8

Cracking in the 45° ply on the outer surface was observed prior to failure in all of the specimens except the specimen with zero prestrain. Examination of the failed specimens revealed that the failure was a mixture of adhesive debonding and a small amount of composite damage in the 45° and 90° plies, as shown in Figure 3.

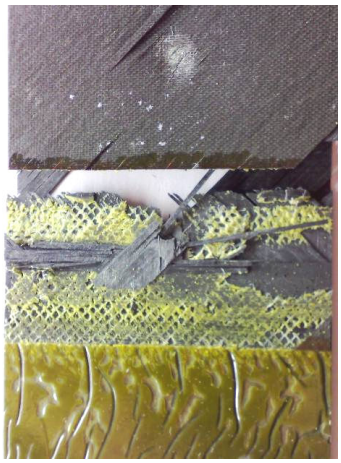

Figure 3: Failed specimen showing debonding and a small amount of composite failure in the 45°and 90° plies

The specimen without prestrain failed in a different manner. Here, pure bondline failure was observed at a relatively low lateral load of 1.6 kN with no indication of composite damage. This might be an indication of a poor bond for this test specimen. The scarf joint opened from the outside surface, accompanied by a significant reduction in the bending stiffness. As the lateral displacement increased, the specimen continued to bend about the loading point without breaking into separate pieces, as shown in Figure 4. The test was subsequently stopped. The failure load for this specimen was

considered to be the maximum force applied immediately prior to the opening of the scarf tip.

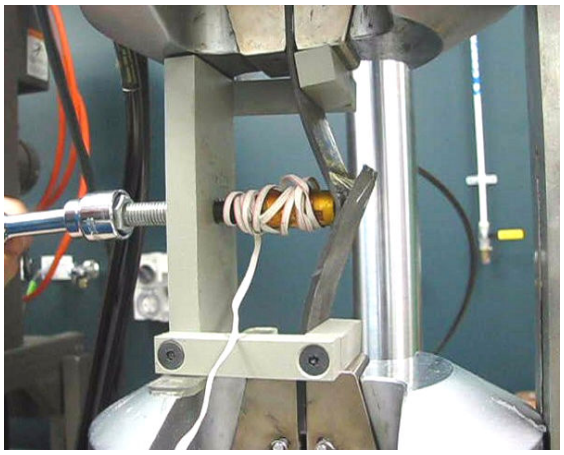

Figure 4: Failure of specimen without prestrain

4 Finite Element Modelling

An advanced FE analysis was undertaken to examine the conditions of prestrain and lateral loading leading to catastrophic failure. The commercial FE code Abaqus 6.7 was used for the analysis. The analysis was split into two steps. Both the preloading step and the lateral loading event were modelled as static events in Abaqus/Standard. All analyses were run by including nonlinear geometric effects and cohesive material degradation for the adhesive.

4.1 Adherends

The scarf joints were modelled with ply-by-ply resolved adherends. A 3-D composite damage model is currently not available in Abaqus, which means that composites ply-by-ply damage cannot be observed with this approach. The numerical predictions therefore deal with adhesive damage only. Alternative approaches to incorporate composite damage are currently under investigation.

Table II presents the ply-by-ply adherend properties. The lay-up is quasi-isotropic, which results in the same properties for the in-plane directions. The material data are based on Cycom T300/970 properties obtained from the manufacturer's data sheets. The composite adherends were modelled with 8-noded Hex elements.

Table II: Adherend Material Properties for FM73

Material property	Value
E_1 [GPa]	120
E_2 [GPa]	8.0
E_3 [GPa]	8.0
G_{12} [GPa]	5.0
G_{13} [GPa]	5.0
G_{23} [GPa]	2.7
ν_{12}	0.45
ν_{13}	0.45
ν_{23}	0.20

4.2 Cohesive Model

Eight-noded 3-D cohesive elements within Abaqus were used to model the adhesive layer. A triangular traction-separation law was applied. The bulk stiffness values K_I and K_{II} correspond to the Young's modulus and shear modulus, respectively. To model the adhesive failure, the power law mixed mode behaviour was chosen:

$$\left(\frac{G_n}{G_I}\right)^2+\left(\frac{G_s}{G_{II}}\right)^2+\left(\frac{G_t}{G_{III}}\right)^2=1$$

Following adhesive failure, the cohesive elements were not deleted to ensure a remaining compressive contact interaction of the two adherends. The material properties presented in Table III were derived from the published experimental data for Cytec FM 73 [9,10].

Table III: Cohesive Material Properties for FM73

Material property	Value
K_I [MPa]	2,200
K_{II} [MPa]	805
K_{III} [MPa]	805
G_I [N/mm]	3.00
G_{II} [N/mm]	6.50
G_{III} [N/mm]	6.50
$\sigma_{ult,\,I}$ [MPa]	55.0
$\sigma_{ult,\,II}$ [MPa]	32.0
$\sigma_{ult,\,III}$ [MPa]	32.0

The cohesive model parameters were verified against static tests of scarf-joints loaded to tensile failure in previous work [6]. Over-meshing was used for the ply-by-ply approach within the adhesive bondline as the element size within the adherends is significantly smaller.

Over-meshing is a versatile approach within Abaqus which allows the mesh density of the adhesive to be different from the mesh density of the adherends; therefore the nodes do not need to coincide. A *TIE constraint is imposed on both interfaces between the adhesive bondline and the respective adherend; thereby assuming perfect bonding between the two. The mesh for the ply-by-ply approach is visualized in Figure 5.

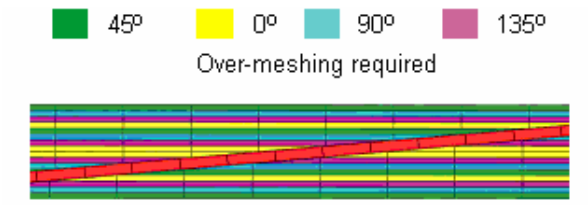

Figure 5: Mesh for the ply-by-ply approach with over-meshing

4.3 Boundary Conditions

In the experimental study, preloading of the specimen occurred under load control. The specimen was allowed to move in tensile loading direction during the lateral loading event. This significantly influenced the bending stiffness of the specimens.

The specimens were deformed laterally at the centre with an impactor with a 12 mm spherical tup. The impactor was modelled as a rigid body as all deformation was assumed to occur in the joint. Small sliding contact conditions were imposed between impactor and composite joint. The sensitivity of the model to the boundary conditions for the application of the lateral load (see Figure 2 for experimental set-up) was investigated in a separate study. Changes in bending stiffness and failure load were found to be negligible for models with and without additional reaction forces from the lateral force rig. The impactor was modelled as displacement controlled to enable capture of the maximum force and force reduction after adhesive failure.

4.4 Finite Element Analysis Results

The numerical load-displacement curves for the varying prestrain values can be seen in Figure 6. The graph also indicates the maximum lateral force and point of first significant adhesive failure. The numerical damage variable indicates complete failure for the elements in the adhesive layer (red regions).

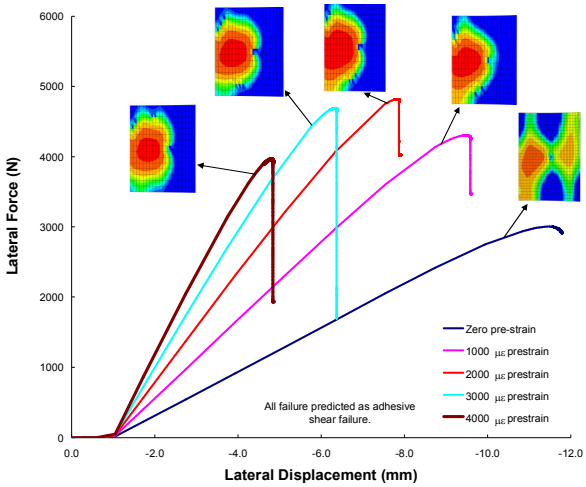

Figure 6: Load-displacement curves for varying prestrains

To validate the applied boundary conditions for prestraining and lateral force, the numerical bending stiffness was compared to the experimental bending stiffness in Figure 7. Both agree well. It is obvious that the bending stiffness increases with increasing prestrain. The bending stiffness increases by a factor of 3.6 for an applied prestrain of 4,000 με.

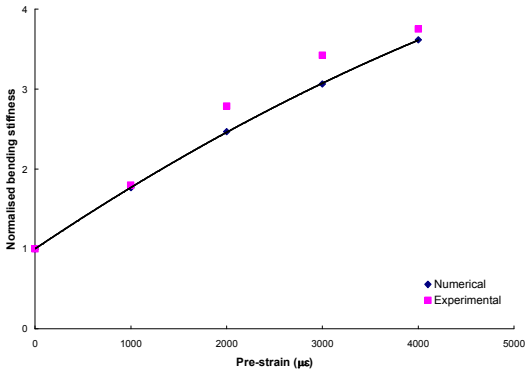

Figure 7: Change in bending stiffness with prestrain

5 Discussion

From the experimental failure of the joints, it was clear that a small amount of composite failure in the 45° and 90° plies was observed in addition to the bondline failure, but the order of failure remains unclear. The adhesive failure predictions result in very good agreement with the experimental failure loads under prestrain as shown in Figure 8.

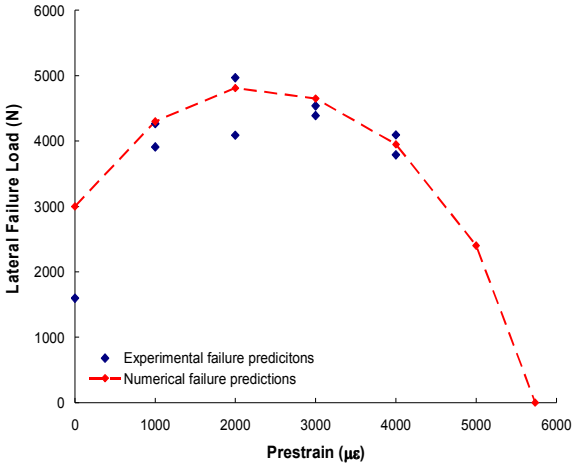

Figure 8: Experimental versus numerical lateral failure load

The strong agreement between the numerical predictions and the experimental results suggests that failure was dominated by the adhesive strength, rather than that of the composite. Although composite damage cannot be modelled in the current analysis (refer Section 4.1), elemental stresses over time were compared to the longitudinal and transverse ply strengths. The longitudinal stresses were found to be significantly below the fibre failure strength in the 0º plies, while transverse stresses suggested that some matrix cracking may have occurred in the tensile loaded 45° and 90º plies near the time of joint failure. Further work needs to be undertaken to incorporate composite failure into the numerical model to investigate all failure modes. Nevertheless, it is believed that debonding plays a dominant role in the failure initiation of scarf joints subject to combined tensile and bending loads. This is largely consistent with the findings of previous impact studies [5,6].

For the zero prestrain specimen, a significant difference was observed between the numerical prediction and the experimental result. The failure load of this specimen was found to be appreciably lower than the theoretical prediction. This may be attributed to the poor interfacial peel strength between the adhesive and the composite substrate. Further work is required to investigate this behaviour.

The lateral failure load firstly increases and then decreases with increasing prestrain, as shown in Figure 6. This indicates that a moderate prestrain (around 2,000 με) is beneficial in terms of the lateral failure load for the static loading case. The failure displacement decreases linearly with the applied prestrain to zero at the tensile failure strain (see Figure 9). This linear dependence clearly shows that the assumption of superposition of bending and tensile strain is valid for quasi-static loading.

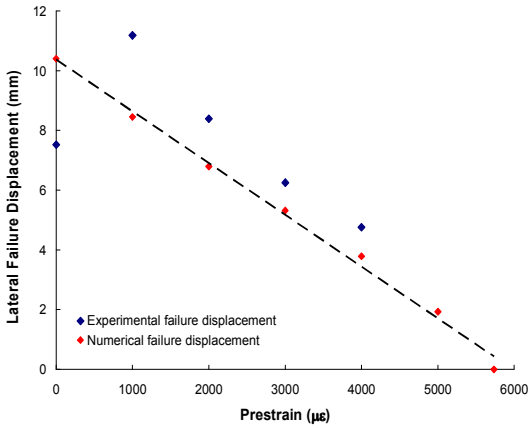

Figure 9: Experimental versus numerical lateral failure displacement

The failure mechanisms observed in this study are largely similar to those found in previous impact studies [5,6], although a slightly greater amount of composite damage was seen in the static tests. The lateral failure loads in the static tests are greater than those found in the impact studies [5,6]. This suggests that the adhesive strength is reduced in the case of dynamic impact events as a result of the high strain rate. Secondary higher-order oscillations in the scarf joint during impact may also give rise to high adhesive stresses compared to the static case. Therefore, the benefit provided by a

moderate prestrain may be negated in the case of dynamic impact. Further studies to measure high strain rate material properties of the adhesive are currently being undertaken.

6 Conclusion

A study was conducted on the behaviour of tensile prestrained 5° quasi-isotropic carbon/ epoxy scarf joints subject to quasi-static lateral loading. It was found that the failure mechanism was predominantly debonding of the adhesive joint with a small amount of composite failure in the 45° and 90° plies. This is consistent with the findings of previous studies on the impact of scarf joints under load. The experimental results agreed well with FE models incorporating cohesive elements to simulate adhesive damage. Failure occurred as a result of the combined stresses from the tensile preload and bending. Both the theoretical and experimental results indicated that a moderate prestrain of around 2,000 με maximised the lateral failure load. However, it is believe that this benefit may be negated in the case of dynamic impact due to the reduction in adhesive strength as a result of the high strain rate and secondary higher mode oscillations.

References

[1] Schweinberg, W., Fiebig J, Adams, S., Armstrong, J., Banks, H. and Brown, C., Bonded composite doubler repair of severely corroded C-130 primary wing structure", *Proc The 4th Joint DoD/FAA/NASA Conference on Aging Aircraft*, 15-18 May, 2000.

[2] Abrate, S., *Impact on composite structures*, Cambridge University Press, 1998.

[3] Reid, S.R. and Zhou, G. (eds), *Impact behaviour of fibre-reinforced composite materials and structures*, CRC Press, Woodhead, 2000, pp. 1-32.

[4] Herszberg, I., Weller, T., Leong, K.H. and Bannister M., The Residual Tensile Strength of Stitched and Unstitched Carbon/Epoxy Laminates Impacted under Tensile Load., *Proc The First Australia Congress on Applied Mechanics*, Melbourne, Australia, Feb 21-23, 1996.

[5] Li, H.C.H., Mitrevski, T. and Herszberg, I., Impact on Bonded Repairs to CFRP Laminates under Load., *Proc The 25th Congress of the International Council of the Aeronautical Sciences*, Hamburg, Germany, 3-8 September 2006.

[6] Herszberg, I., Feih, S., Gunnion, A.J. and Li, H.C.H., *Impact damage tolerance of tension loaded bonded scarf repairs to CFRP laminates*, 16th International Conference on Composite Materials, Tokyo, Japan, July 2007.

[7] Baker, A.A., Dutton, S. and Kelly D., *Composite Materials for Aircraft Structures*., AIAA Inc, Reston, 2004.

[8] Soutis, C. and Hu, F.Z., Strength Analysis of Adhesively Bonded Repairs, in Tong, L. and Soutis, C. (eds), *Recent Advances in Structural Joints and Repair for composite Materials*, Kluwer Academic Publishers 2003, pp 141-172.

[9] Chalkley, P. and van den Berg, J., On obtaining design allowables for adhesives used in the bonded-composite repair of aircraft, DSTO-TR-0608, Defence Science and Technology Organisation, Melbourne, Australia, 1997.

[10] Gunnion A.J. and Herszberg I., Parametric study of scarf joints in composite structures, *Journal of Composite Structures*, 75(1-4):364-376, 2006.

Copyright Statement